MRI SLICE SELECTION WITH SCALING FUNCTIONS

Juan José Vaquero, Andrés Santos, Francisco del Pozo
Grupo de Bioingeniería y Telemedicina, E.T.S.I. Telecomunicación (U.P.M.)
28040 Madrid, Spain.   e-mail: jjvl@teb.upm.es

Abstract — A new family of amplitude–only radiofrequency modulation waveforms for slice selection in Magnetic Resonance Imaging (MRI) is presented. Based on the scaling functions associated to different wavelet families, these new envelope waves provide higher slice selectivity than gaussian or sinc functions. They are also more compact on the time domain, since no truncation is needed, allowing to reduce the time required for the slice selection process. This feature is valuable on multislice-multiecho and fast acquisitions. Their performance has been evaluated both through simulations of the Bloch equations, and by measuring the slice width of real ramp phantoms images. The simulation results show that this amplitude modulation causes a phase behaviour of the resonant protons within the selected volume that is more coherent than with other techniques. This effect can be related to the higher intensity of the images acquired with this slice selection procedure.

I. INTRODUCTION

Many MRI techniques require slice selection using short radiofrequency (RF) pulses applied simultaneously with a magnetic field gradient across the object to be explored. The pulse selectivity can be measured by quantifying the resonance slice profile. Hoult (1) demonstrated that the evaluation of this selection profile by the Fourier transform (FT) method can only be accepted for soft (low angle) pulses, due to the non-linear response of the spin magnetisation. It is widely accepted however that narrow slice profiles can be achieved by lengthening the RF pulse. Phase dispersal is another effect that limits the reliability of the FT analysis: after the excitation pulse, the phase of the different spins are spatially-dependent distributed, and a refocussing gradient is needed to compensate this undesired effect. An accurate evaluation of the phase dispersion originated by the excitation pulse is also highly desired.

Modern pulse design includes different alternatives (2-6), providing envelopes that in some cases need both, amplitude and phase modulation. A requirement of our work was the use of RF pulses with only amplitude modulation, due to hardware limitations of the systems for which they were designed. Then, in a first stage the excitation profile created by a scaling function envelope was analyzed with computer simulations of the Bloch equations using a Runge-Kutta integration method. That provided exact theoretical results (7). An additional experiment was carried out by measuring slice thickness on phantom images.

II. MATERIALS AND METHODS

In (9), Mallat described a method for computing the wavelet transform of a signal, using the *wavelet* $\psi(x)$ and *scaling* $\phi(x)$ functions, which are closely related; from (8,9) it is well known that if $\phi(x)$ is a scaling function, then an orthonormal basis of $L^2(R)$, the vector space of measurable, square-integrable one dimensional functions, can be defined as

$$\left(\sqrt{2^{-j}} \cdot \Phi_{2^j}(x - 2^{-j \cdot n}) \right)_{n \in Z}$$

Consequently $f(x) \in L^2(R)$ can be approximated by an expression that uses this basis. If we define a filter H as

$$h(n) = \left\langle \phi_2^{-1}(u), \phi(u - n) \right\rangle = \int_{-\infty}^{\infty} \frac{\phi(u/2)}{2} \cdot \phi(u - n) \cdot du \quad \forall n \in Z$$

and $\tilde{H}$ is the mirror filter of H, defined as $\tilde{h}(n) = h(-n)$, the previous $f(x)$ expansion can be written as

$$\left\langle f(u), \phi_2^{-1}(u - 2 \cdot n) \right\rangle = \sum_{k=-\infty}^{\infty} \tilde{h}(2 \cdot n - k) \cdot \left\langle f(u), \phi_2^{j+1}(u - 2^{-j-1} \cdot k) \right\rangle$$

that is the convolution of $\tilde{H}$ with the previous approximation of $f(x)$, followed by a decimation. The filter H can be written as a discrete expansion on Fourier terms. If $|H(\omega)| \neq 0$, and $\omega \in [0, \pi/2]$, the Fourier transform of the scaling function is given by

$$\hat{\Phi}(\omega) = \prod_{p=1}^{\infty} H(2^{-p} \cdot \omega)$$

The same procedure that has been applied to the scaling function, can be used to define a new function $\psi(x)$ (the wavelet)

$$\hat{\Psi}(\omega) = G(\frac{\omega}{2}) \cdot \hat{\Phi}(\frac{\omega}{2})$$
$$G(\omega) = e^{-j\omega} \cdot \overline{H}(\omega + \pi)$$

whose family of dilations and translations

$$\left(\sqrt{2^{-j}} \cdot \Psi_{2^j}(x - 2^{-j \cdot n}) \right)_{n \in Z}$$

constitutes also an orthogonal base of $L^2(R)$ (9). Daubechies demonstrated that it is possible to find H so that $\psi(x)$ and $\phi(x)$ are zero outside a finite interval in the x axis; these functions will have finite support in time and frequency domain. Based on this property, a set of selective RF pulses has been implemented by using as envelopes the scaling functions; wavelets cannot be used as their integrals, by definition, are zero, and so the final flip angle will always be zero. Daubechies scaling functions (figure 1) have been chosen due to their finite support and smooth shape; they need only amplitude modulation, as we required.

The performance of these slice selection functions is compared against conventional gaussian pulses, sinc-gaussian pulses (a sinc-shaped modulator pulse that has been smoothed with a gaussian filter function) and hermitian pulses.
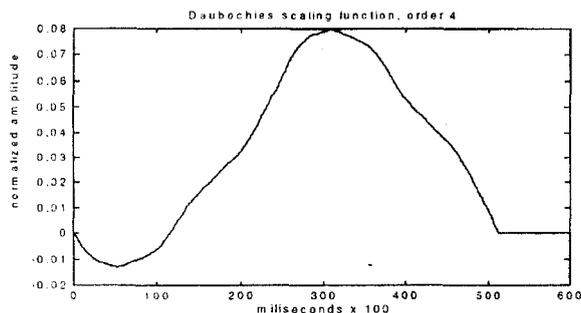
1

Figure 1: scaling function used as radiofrequency selective pulse envelope.

Images for slice thickness measurements have been acquired in two different systems, in both limiting the length of the pulse to 256 real points (6):

1. A whole body 0.12 tesla prototype made by NESA-ITISA (Granada-Madrid, Spain), using a low-intensity ramps phantom. The envelope waveform was recorded on the modulator EPROM, substituting the original gaussian-sinc. RF amplifier gain was adjusted manually by measuring the flip angle of the excitation.

2. A 4.7 tesla Bruker Biospect system. Pulses were programmed downloading the waveform on the main console in polar form. The dynamic range was 1K for the amplitude and 4K for the phase. A total of 256 complex points, with the phase set to zero, was used. The system adjusted automatically the RF amplifier gain.

Images were acquired with spin-echo and fast spin-echo sequences, and different echo-time (TE) and repetition time (TR).

III. RESULTS AND DISCUSSION

Simulation results have been compared by measuring the *full width half maximum* (FWHM) of the slice profile generated with the proposed scaling function, on different experiments: a) scaling function compared to gaussian pulses

(10); b) scaling functions at different scales, c) scaling functions versus gaussian-sinc pulses, and d) scaling functions versus hermitian pulses. In all cases the results have been evaluated for 90° and 180° flip angles. Phase has also been analysed since it gives an estimation of pulse coherence.

In all cases scaling function pulses outperform the others, both in selectivity and phase linearity. Table 1 shows part of the quantified results for different simulations.

Pulse duration	2,56 ms	1,28 ms	0.64 ms
90°	30 %	65 %	135 %
180°	33 %	60 %	127 %

Table 1: FWHM variation quantification for different duration scaling functions, rated to a gaussian-sinc 2,56 milliseconds pulse.

Real slice profile ratio between the scaling function and gaussian-sinc pulses (both of the same duration) has been quantified in 56%; this deviation from the simulation results is due to several well known reasons, being the most relevant the prototype main field non-homogeneity, partial volume effect and system noise.

IV. REFERENCES

1. Hoult, D.I. , *J. Magn. Reson.* 35, 69-86, 1979.
2. Silver, M.S., Joseph, R.I., Hoult, D.I., *J. Magn. Reson.* 59, 347-351, 1984.
3. Shinnar, M., Eleff, S., et al., *Magn. Reson. Med.* 12, 74-80, 1989.
4. Mao, J., Virapongse, C., et al., *Magn. Reson. Med.* 13, 293-298, 1990.
5. Buonocore, M.H., *Magn. Reson. Med.* 29, 470-477, 1993.
6. Slotboom, J., Creyghton, J., et al., *Magn. Reson. Med.* 30, 732-740, 1993.
7. Locher, P.R., *Phil. Trans. R. Soc. Lond.* B 289, 537-542, 1980.
8. Daubechies, I., *IEEE Trans. Info. Theory* 36, 5, 961-1005, 1990.
9. Mallat, S., *IEEE Trans. Pattern Anal. Machine Intell.* 11, 679-693, 1989.
10. Bauer, C., Freeman, R., et al., *J. Magn. Reson.* 58, 442-457, 1984.
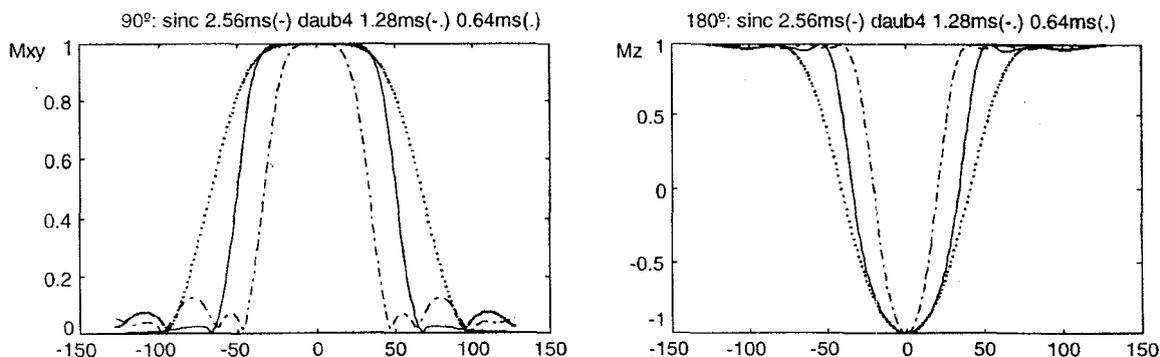
Figure 2: final magnetisation across the slice for different 90° (*left*) and 180° (*right*) flip angle pulses, using the scaling function and gaussian-sinc envelopes, with several durations: 2.56 ms gaussian-sinc (solid), 1.28 ms scaling function (dashed) and 0.64 ms scaling function (dotted). Vertical axis is the normalised magnetisation; horizontal axis is the distance to the slice centre, in arbitrary units.